Journal of Structural Biology 183 (2013) 467–473

Contents lists available at SciVerse ScienceDirect

Journal of Structural Biology

journal homepage: www.elsevier.com/locate/yjsbi

Single-cell lysis for visual analysis by electron microscopy

Simon Kemmerling [a,1], Stefan A. Arnold [a,1], Benjamin A. Bircher [a], Nora Sauter [a], Carlos Escobedo [b], Gregor Dernick [c], Andreas Hierlemann [b], Henning Stahlberg [a], Thomas Braun [a,*]

[a] Center for Cellular Imaging and Nano Analytics (C-CINA), Biozentrum, University of Basel, Basel, Switzerland
[b] Bio Engineering Laboratory (BEL), Department of Biosystems Science and Engineering (D-BSSE), ETH Zurich, Basel, Switzerland
[c] Discovery Technologies, Pharma Research and Early Development (pRED), F. Hoffmann-La Roche AG, Basel, Switzerland

ARTICLE INFO

Article history:
Received 6 February 2013
Received in revised form 20 June 2013
Accepted 24 June 2013
Available online 29 June 2013

Keywords:
Electron microscopy
Microfluidics
Single-cell analysis
Single-cell lysis
Systems biology

ABSTRACT

The stochastic nature of biological systems makes the study of individual cells a necessity in systems biology. Yet, handling and disruption of single cells and the analysis of the relatively low concentrations of their protein components still challenges available techniques. Transmission electron microscopy (TEM) allows for the analysis of proteins at the single-molecule level. Here, we present a system for single-cell lysis under light microscopy observation, followed by rapid uptake of the cell lysate. Eukaryotic cells were grown on conductively coated glass slides and observed by light microscopy. A custom-designed microcapillary electrode was used to target and lyse individual cells with electrical pulses. Nanoliter volumes were subsequently aspirated into the microcapillary and dispensed onto an electron microscopy grid for TEM inspection. We show, that the cell lysis and preparation method conserves protein structures well and is suitable for visual analysis by TEM.

1. Introduction

The aim of systems biology is to understand the emergence of biological functions from interaction networks (Westerhoff, 2011). This requires knowledge of the intracellular players and their interconnections, for which an inventory of the individual components of the system, i.e. the transcriptome, the proteome, the metabolome and, finally, the interactome, has to be assembled. Such an inventory will strongly vary from cell to cell, as the stochastic nature of biological processes leads to "biological noise" (Eldar and Elowitz, 2010; Raj and van Oudenaarden, 2008). This makes the study of individual systems, e.g., single cells, a necessity (Wang and Bodovitz, 2010).

Genome sequencing (Zong et al., 2012) and expression profiling (Flatz et al., 2011) are far advanced, and amplification techniques are ready to be applied to single cells (Kalisky et al., 2011). The analysis of the metabolism of a biological system profits from the experience and advances of analytical chemistry (Fiehn, 2001); for example, mass spectrometry (MS) can be used to identify metabolites with single-cell sensitivity (Amantonico et al., 2008). Moreover, excellent imaging techniques, such as light- and electron microscopy (EM) or X-ray diffraction imaging, are available for structural analyses.

However, proteomic studies at the single-cell level are hampered by the low expression level of many proteins and the lack of amplification techniques. Although powerful and valuable techniques, such as MS (Picotti et al., 2009) and cryo-electron tomography (cryo-ET) (Henderson et al., 2007; Medalia et al., 2002; Nickell et al., 2006), are applied for single-cell proteomic studies, such studies still remain a challenging task, especially for eukaryotic cells (Bantscheff et al., 2007; Diebolder et al., 2012; Mader et al., 2010). Thus, adjuvant techniques utilizing novel or hybrid approaches are beneficial to further untangle the complexity of single-cell protein networks.

A combination of microfluidics and TEM was suggested as an alternative and complementary approach to investigate the protein content of single eukaryotic cells (Engel, 2009, 2010). The idea is to

Abbreviations: AM, ammonium molybdate; BHK, baby hamster kidney; ddH_2O, double-distilled water; ECL, enhanced chemiluminescence; EM, electron microscopy; ET, electron tomography; FEA, finite element analysis; FS, fused silica; HRP, horseradish peroxidase; ID, inner diameter; ITO, indium tin oxide; MS, mass spectrometry; OD, outer diameter; OM, optical microscope; PDMS, poly(dimethylsiloxane); PEEK, poly(ether–ether–ketone); RPPA, reverse-phase protein arrays; SNR, signal-to-noise ratio; TEM, transmission electron microscopy; UA, uranyl acetate.

* Corresponding author. Address: C-CINA, Mattenstrasse 26, CH-4058 Basel, Switzerland. Fax: +41 (0)61 387 39 86.
E-mail address: thomas.braun@unibas.ch (T. Braun).

[1] These authors contributed equally to this work.

1047-8477
http://dx.doi.org/10.1016/j.jsb.2013.06.012

physically lyse single cells and spread the entire sample onto EM grids for structural analysis by transmission electron microscopy (TEM), or mass measurements by scanning TEM (STEM). This "lyse and spread" approach provides access to EM imaging at a higher signal-to-noise ratio (SNR) than when in the cellular background, and enables a more straightforward correlation of structural information with mass data. A prerequisite of this envisaged approach is a targeted lysis of individual cells and an efficient preparation of their lysate for TEM analysis.

A variety of different techniques for single-cell lysis exists today, and most of them have been implemented in microfluidic systems (Brown and Audet, 2008). Many of these systems utilize the principle of electroporation (Fox et al., 2006; Movahed and Li, 2011) to lyse detached or suspended cells in flow-through configurations, whereas only a few report on electrical lysis of "standard" adherent eukaryotic cells in cultures (Han et al., 2003; Nashimoto et al., 2007). However, despite their popularity none of these systems has been utilized to prepare samples of a single-cell lysate for electron microscopy.

Here, we present a system for the electrical lysis of individual adherent eukaryotic cells and subsequent preparation of minute sample volumes for negative-stain TEM. The setup includes a custom-designed microcapillary electrode (Fig. 1), which targets and lyses individual cells observed in a light microscope. Immediately after lysis, the cell-fragments are aspirated into the microcapillary, deposited on an EM grid and negatively stained. This method offers the potential for an alternative approach to analyze proteins and protein complexes from individual eukaryotic cells.

2. Materials and methods

2.1. Instrument setup

The principle and basic design of the system developed for the electrical lysis of single cells is shown in Fig. 1 A. The system is designed for use with an inverted optical microscope (OM; Zeiss Axiovert 40C). The microscope is equipped with a custom-built stage that has a customized mounting frame on the objective guide. The latter accommodates an indium tin oxide (ITO)-coated glass slide (ground electrode and sample platform) and can be moved manually in the xy-plane. Miniaturized Petri dishes on the surface of the glass slide (see below) allow cell cultures to be grown. A tapered gold-coated microcapillary that serves as second electrode can be positioned in close proximity above the glass slide. The upper un-tapered end of the microcapillary is inserted in a steel adapter and electrically connected with silver paint (Fig. 1B). The insulating holder of the adapter is attached to a stepper motor (PI M-126.PD2, Physik Instrumente, Germany) mounted on top of an xy-platform on the microscope stage. This platform allows the microcapillary tip to be centered above the objective lens of the OM. The stepper motor moves the capillary in the z-direction. The other end of the steel adapter holding the capillary is connected via a PEEK (poly(ether–ether–ketone)) tube (inner diameter (ID) 250 μm) to a pressure reservoir (Fig. 1). The tube is intercepted by a solenoid valve (LVFA0550310H, The Lee Company, USA) that is controlled by the computer through an NI USB-6009 module. A pressure controller (PCNC-0001-00, Seyonic, Switzerland) is used to apply positive or negative pressure to the system via the pressure reservoir. A function generator (33220A, Agilent, Switzerland) delivers a voltage signal, which is amplified 20 times by a linear voltage amplifier (F20A, FLC Electronic AB, Sweden). The output of the linear amplifier is electrically connected to the capillary, and the conductive glass slide is grounded. All electronic components of the system are controlled by a LabVIEW-based, custom-made software (Supp. Fig. 1). A camera (GC750 GigE, Prosilica, USA), mounted on the microscope, enables live-cell imaging and video recording. The next version of the control software will be available as an open-source plug-in for the openBEB (open biological experiment browser) system (www.openBEB.org).

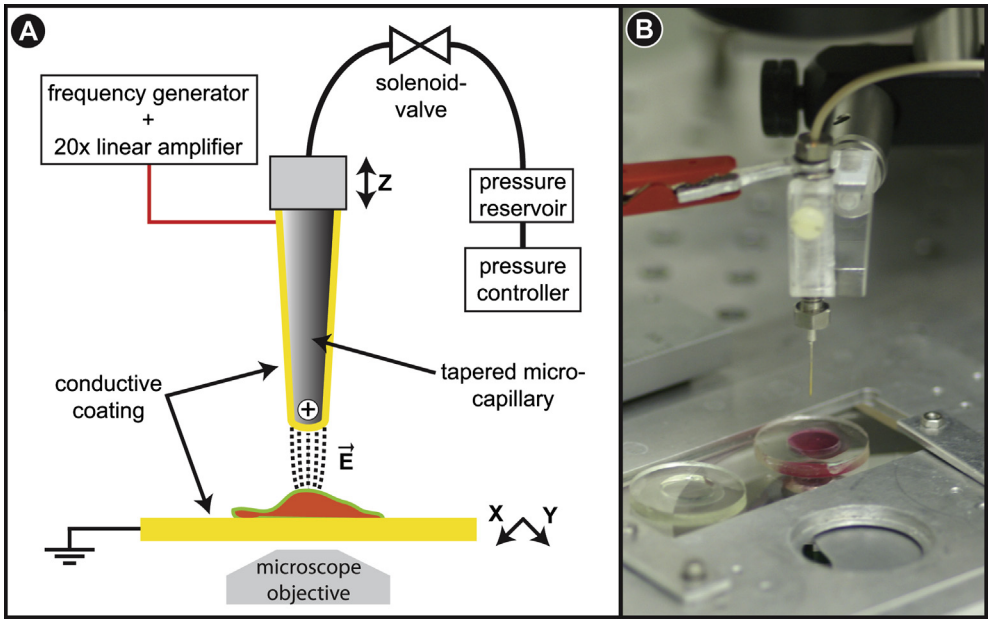

Fig.1. Single-cell lysis instrumentation. (A) Schematic representation of the single-cell lysis setup, which is mounted on an inverted optical microscope. A camera allows for live-cell imaging. The stepper motor approaches the gold-coated microcapillary to the ITO-coated glass slide, where individual cells can be targeted. The function generator sends a voltage pulse to the capillary tip to lyse the cell. Meanwhile, the pressure controller builds up a negative pressure on the closed solenoid valve. Upon cell lysis, the valve is opened for a defined period of time, and the cell lysate is aspirated into the capillary. (B) Lysis microcapillary and cell culture slide. The upper end of the gold-coated microcapillary is inserted into a steel adapter and electrically connected with silver paste. The other end of the steel adapter is attached to a piece of PEEK tubing that connects the microcapillary to the pressure controller via a pressure reservoir. The microcapillary is positioned above a grounded, ITO-coated, glass slide with a PDMS ring on its surface. Slide and ring form a mini Petri dish that can be filled with cell culture medium (red).

2.2. Microcapillaries

Fused-silica (FS) microcapillaries (outer diameter (OD) 350 μm, ID 250 μm, Polymicro) were cut to a length of 10–15 cm. The polymer coating in the middle was removed over a length of 1–2 cm, using hot chromic-sulfuric acid (102499, Merck, Switzerland). Afterwards, the microcapillaries were rinsed thoroughly with double distilled H_2O (ddH_2O), followed by isopropanol and subsequently pulled with a laser-based micropipette puller (Sutter Instruments, P2000) to obtain a taper with a 30–50 μm ID at the tip. The tapered microcapillaries were plasma-cleaned before the sputter-deposition of a 2 nm Ti adhesive layer, followed by a 50–100 nm Au layer on their outer surface to increase conductivity. Coating was successively performed from two opposite sides at an angle of 45 degrees to obtain a closed conductive layer around the microcapillaries.

2.3. Miniaturized Petri dishes on conducting glass slides

Commercially available ITO-coated glass slides (Diamond Coatings UK, 8–12 Ω/square) were used as a conductive substrate for cell culturing. These slides have a silver electrode at each end for electrical connections. They were washed and sonicated in detergent solution (1% Alconox, Alconox Inc., USA), rinsed with ddH_2O and stored in ethanol until use.

PDMS (poly(dimethylsiloxane), Dow Corning SYLGARD 184) rings with an ID of 1 cm and a height of 2–3 mm, were fabricated and reversibly bonded onto glass slides to form sample wells with a volume of about 250 μl. These miniaturized Petri dishes allowed cells to be grown and kept in a physiological buffer solution during the experiment. An ITO glass slide with a PDMS ring filled with cell culture medium is shown in Fig. 1B.

2.4. Cell culture

Adherent baby hamster kidney fibroblasts (BHK21; ECACC 85011433) were cultured in polystyrene T75-flasks containing 30 ml DHI-5 medium (see below) at 37 °C and 5% carbon dioxide. To split the cells, the medium was removed, and the flask was washed with 10 ml of 37 °C warm PBS w/o calcium and magnesium (Dulbecco's Phosphate Buffered Saline, D8537, Sigma, Switzerland). To detach the cells, 3 ml of trypsin–EDTA solution (0.05% Trypsin, 0.53 mM EDTA; 25300-054, Invitrogen, Switzerland) were added, and the cells were incubated at 37 °C for 5 min. The detached cells were diluted with 7 ml of 37 °C warm DHI-5 medium and homogenized using a pipette. 0.5 ml of the homogenized cell suspension and 30 ml of fresh media were returned to the flask for further cultivation. The rest of the cell suspension was used for experiments or disposed. A miniaturized Petri dish was filled with approximately 250 μl of medium, and 1–2 μl of cell suspension were added. The cells were incubated on the glass slide base of this dish for 1–2 days at 37 °C and 5% CO_2.

DHI-5 medium is a 1:1:2 mixture of DME (Dulbecco's Modified Eagles Medium; D6171, Sigma, Switzerland), HamF12 (Nutrient Mixture F-12Ham; N8641, Sigma, Switzerland), and IMDM (Iscove's Modified Dulbecco's Medium; I3390, Sigma, Switzerland) media, supplemented with 5% FCS (Fetal Bovine Serum; E7524, Sigma, Switzerland) and complemented with non-essential amino acids (MEM non-essential amino acid solution; M7145, Sigma, Switzerland), L-glutamine (L-glutamine solution; G7513, Sigma, Switzerland), and vitamins (RPMI1640 vitamins solution; R7256, Sigma, Switzerland).

For the single-cell lysis experiments, the medium was removed from the sample well, and the cells were washed twice with 37 °C warm PBS (Dulbecco's Phosphate Buffered Saline; D8662, Sigma, Switzerland), ISB (isotonic sucrose buffer: 0.25 M sucrose, Bio-Rad, 161–0720; 5 mM HEPES pH 7.4, AppliChem A3724) or HEPES buffer (0.15 M NaCl; 20 mM HEPES pH 7.4; 5.5 mM KCl; 2 mM CaCl2; 1 mM $MgCl_2$). The cells remained in the wash buffer solution during the experiment.

2.5. Cell lysis

Live BHK21 cells were lysed *in situ* in PBS, HEPES or ISB buffer. During the experiments, the conductive glass slide hosting the cell culture was electrically grounded, and the microcapillary was connected to a function generator. The miniaturized Petri dish, formed by a PDMS ring and the glass slide, was positioned on the OM stage. An individual cell was then selected and centered in the field of view with the help of the microscope. Next, the tip of the gold-coated microcapillary was immersed in the buffer solution, brought in close proximity to the conductive surface of the glass slide (distance ≈20 μm) using the stepper motor and aligned directly above the targeted cell by moving the microscope stage. A camera mounted on the microscope allowed for live-imaging of the individual cells and their surroundings during the following lysis procedure. After aligning the microcapillary tip above a targeted cell, a burst of five to ten DC square pulses with amplitudes of 6–10 V and a frequency of 10 kHz (pulse duration: 50 μs) was applied to the gold-coated microcapillary using the function generator. This generated a strong electric field (3–5 kV/cm) across the selected cell and resulted in cell lysis. Note, for the compensation of electrode aging, higher voltages were applied in rare cases (maximally 20 V). Right after the burst, the solenoid valve was opened toward the partially evacuated pressure reservoir (Fig. 1A) and remained open for a defined period of time, aspirating sub-microliter volumes (200–400 nl) of lysate and buffer into the microcapillary. The amount of sample aspirated was controlled by the pressure difference (−50 to −600 mbar) and the opening time of the solenoid valve (50–400 ms). To transfer the sample, an EM grid was clamped by tweezers and centered under the microcapillary. The tip of the microcapillary was approached close to the surface of the grid by the stepper motor. The aspirated sample was then dispensed directly onto the carbon film of the grid by applying a positive pressure to the microcapillary.

Single-cell lysis and aspiration experiments were also performed with fluorescently stained HEK293 cells (see Supplementary material and Supplementary movie 1 and 2).

2.6. Electron microscopy

Loaded sample grids were incubated for 60 s–20 min in a humidity chamber to prevent desiccation. Grids with adsorption times of longer than 3 min were washed on four drops of ddH_2O and blotted once at the end and air-dried. All samples were negatively stained with two 5 μl drops of 2% uranyl acetate (UA) or 2% ammonium molybdate (AM) and imaged in a Phillips CM10 electron microscope operated at 80 kV. The images were recorded on a 2 k × 2 k CCD camera (Olympus SIS, Münster, Germany).

2.7. Enzyme activity assay

Horseradish peroxidase (HRP) conjugated goat anti-mouse IgG (8.5 mg/ml, A2554, Sigma, Switzerland) was diluted to a concentration of 4.25 μg/ml in PBS. 3 μl of the sample was placed onto an ITO coated glass slide, and the microcapillary electrode was placed in the drop, about 20 μm above the glass slide. Different voltages (0 V, 4–18 V in 2 V steps and 22 V), each with a burst count of 5 and a single pulse length of 50 μs were applied. 2 μl were removed from the treated sample droplet, diluted to 8.5 ng/ml in PBS, and the enzymatic activity of HRP was analyzed by enhanced chemiluminescence (ECL) on a dot plot (Amersham ECL

Prime Western Blotting Detection Reagent; RPN2232, GE Healthcare, UK).

3. Results

The single-cell lysis setup (Fig. 1) allows for live-cell imaging, lysis of single adherent eukaryotic cells, rapid aspiration of the lysate, and transfer of the sample onto EM grids. This is demonstrated using adherent BHK21 cells.

The adherent cells were individually lysed *in situ* in buffer solution, while the process was monitored by means of optical microscopy. To achieve lysis, a gold-coated microcapillary tip was positioned in close proximity to and directly above the selected BHK21 cell growing on the ITO coated glass slide inside of a miniaturized Petri dish (Fig. 1B). The distance between the capillary tip and the conductive surface of the glass slide was approximately 20 μm; there was no direct cell contact. As documented by light microscopy, the electric field, generated across the cell by a burst of five to ten 50 μs DC square pulses with amplitudes of 6–10 V applied to the microcapillary electrode, was sufficient to reproducibly and efficiently lyse the BHK21 cells in PBS or HEPES buffer (Fig. 2A–C). Electrical pulses alone were sufficient to achieve lysis as indicated by a necrotic morphology of the targeted cells, nevertheless, cells

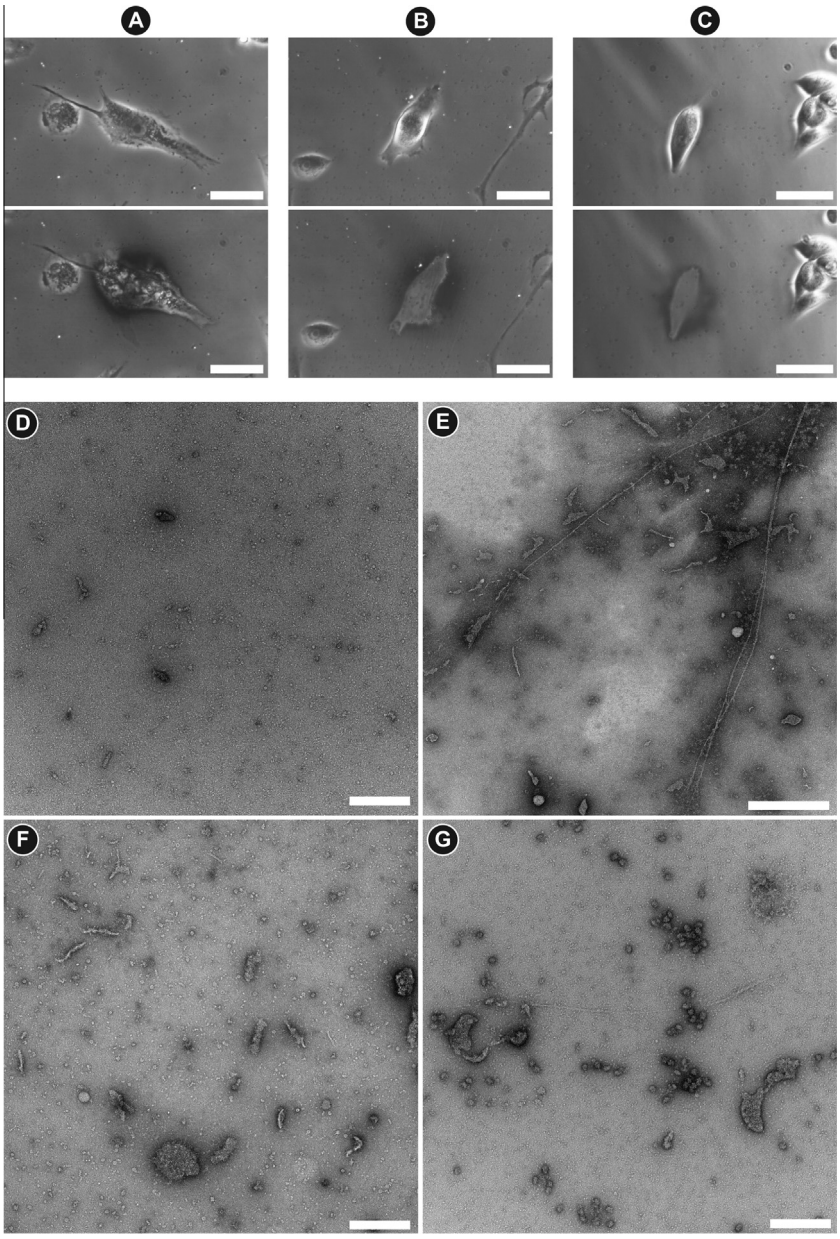

Fig.2. Single-cell lysis and lysate analysis. (A–C) Phase contrast light microscopy images of individual adherent BHK21 cells in PBS (A and B) and HEPES (C) before (top row) and after (bottom row) different procedures. Scale bars: 50 μm. (A) After applying electrical pulses (5 × 50 μs, 10 V DC), the targeted cell is not completely disintegrated but shows necrotic morphology. (B and C) After applying electrical pulses (B: 10 × 50 μs, 6 V DC; C: 5 × 50 μs, 10 V DC) with aspiration, only a ghost imprint of the targeted cell remains; the surrounding cells are not affected (bottom row). (D) Overview TEM image of PBS aspirated from the cell culture well after the washing steps but before a cell lysis event. Such control experiments showed predominantly small particles, but distinctive particles and structures were not detected. Negative stain: 2% UA, Scale bar: 200 nm. (E) TEM image of the aspirated lysate of a single cell showing some μm-long filament and membrane patches. Negative stain: 2% AM. Scale bar: 500 nm. (F) TEM image of the aspirated lysate of a single cell showing some membrane structures, helical filaments and particles resembling the shape and dimensions of Hsp60 and the 20s proteasome. Negative stain: 2% UA. Scale bar: 200 nm. (G) TEM image of the aspirated lysate of a single cell showing membrane structures. Negative stain: 2% UA. Scale bar: 200 nm.

were not completely disrupted, and cell fragments stayed in place if not aspirated (Fig. 2A and Supp. Fig. 2A). Moreover, aspiration alone was not sufficient to lyse, disrupt or detach cells.

As demonstrated, only the targeted cell is lysed and neighboring cells remain unaffected, due to the small electrode dimensions and when conductive buffers are used (Fig. 2A–C and Supp. Fig. 2 A–D). This findings are supported by finite-element analysis (FEA) results, which show that a high electric field is only generated in very close proximity to the cell, between the microcapillary tip and the ITO support (Fig. 3A). Further, adaptation of the electrical parameters to obtain a higher peak-voltage and longer pulse duration allowed the cells to be lysed in low-conductivity, isotonic sucrose buffers, but in this case neighboring cells were also affected (Supp. Fig. 2 E and F).

FEA was also used to estimate the maximal temperature increase by Joule heating due to five 50 µs DC square pulses with amplitudes of 10 V. This estimation predicts a maximal local temperature of 34 °C for a time span of less than 1 ms (Fig. 3 B and Supp. Fig. 3 and 4). The average cell temperature stays below 30 °C throughout the overall time span used for simulation. To experimentally study the effects of the short temperature increase, the enzymatic activity of horseradish peroxidase (HRP) after applying electrical pulses was quantified. HRP is known to be irreversibly impaired by exposition to increased temperatures ((Chattopadhyay and Mazumdar, 2000) and Supp. Fig. 5). Fig. 3C shows the normalized activity of HRP after exposing 3 µl droplets to electrical pulses of different voltages. The effect was measured by quantification of the chemoluminescent reaction catalyzed by HRP. Our results show, that the activity is not significantly decreased below 10 V, but effects are clearly seen around 14 V and higher. Similar experiments performed with synthetic filamentous actin did not reveal signs of protein aggregation or structural damage of the filaments below 10 V (Supp. Fig. 6).

Immediately after the applied burst, lysate and surrounding buffer were aspirated into the microcapillary to prevent diffusion of the cellular content.

Subsequent to cell lysis and aspiration, the sub-microliter volumes (200–400 nl) were loaded onto EM grids, negatively stained and inspected by TEM.

TEM images of buffer solution, aspirated from the miniaturized Petri dish in the proximity of a cell after the washing steps, but before a cell lysis event, showed a background of predominantly small particles as expected (Fig. 2D); these are most likely residues from the growth medium that were not removed by the buffer washes (see Section 2). TEM images of the sample aspirated from the immediate proximity of an individual adherent BHK cell directly after lysis, reveal cellular content (Fig. 2E–G, Fig. 4). Membrane patches, filaments and other structures with distinctive shapes can be recognized and correlated to the specific cell using the light microscopy information. Further examples of prominent structures observed in the lysate of single cells are shown in Fig. 4. Although the control experiments documented the presence of some (predominantly small) particles in the bare buffer solution (Fig. 2D), distinctive structures similar to those found in the lysate (Fig. 2E–G and Fig. 4) were not detected.

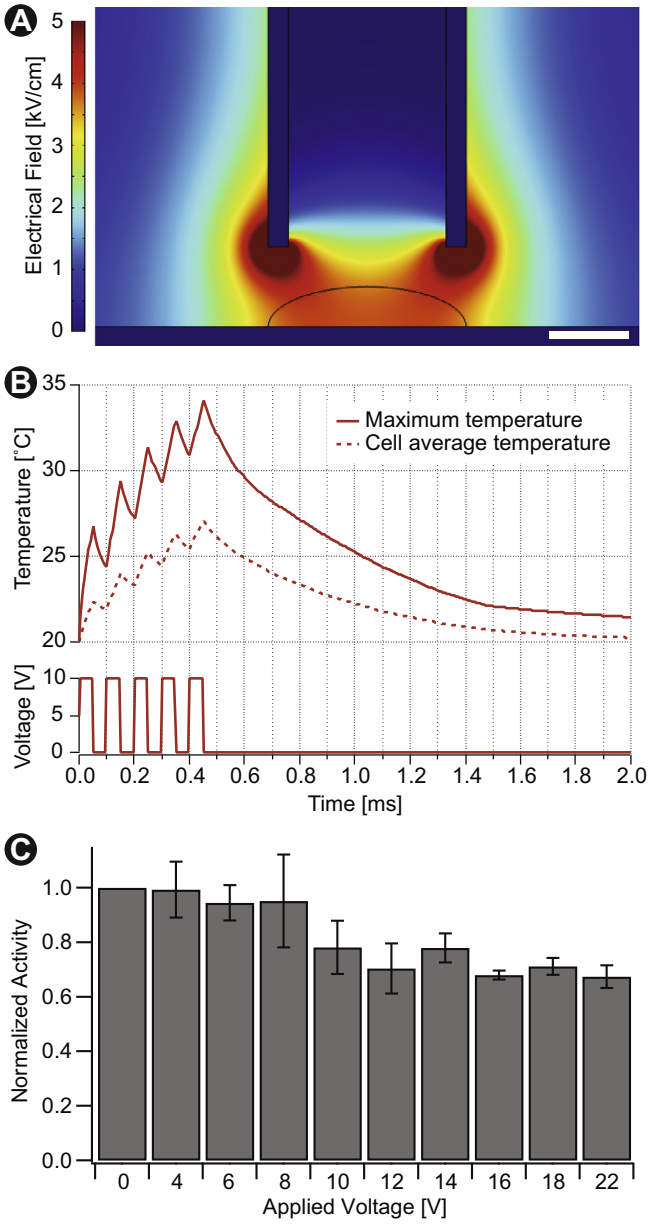

Fig.3. Finite element analysis (FEA) of electroporation characteristics and data on horseradish peroxidase (HRP) stability. (A) FEA simulation to estimate the electric field strength (kV/cm); Scale bar: 20 µm. A potential of 10 V was applied to the microcapillary electrode immersed in PBS buffer; the inter-electrode distance was 20 µm. The profile of a cell (curved black line) placed on the bottom electrode (ITO) was added to the model for illustration. (B) Estimated temperature changes predicted by FEA. The solid line (top panel) shows the variation of the maximum temperature in the solution over time as result of electric pulses (10 V) applied via the gold-coated microcapillary. The dotted line shows the average temperature within the cell region, depicted as curved black line in panel A. (C) Voltage dependence of HRP activity after applying electric pulses. The activity was normalized to that of the control experiments (0 V).

4. Discussion

We present a setup for the controlled lysis of single, adherent eukaryotic cells and a subsequent visual inspection of cellular components by negative-stain TEM. The developed instrument enables (i) live-cell monitoring before and during cell lysis by optical microscopy, (ii) precise selection of individual cells, (iii) fast lysis (<500 ms) without prior disturbance of the cell and (iv) immediate aspiration of the cellular components into a microcapillary for further treatment.

The ITO coating on the glass slide that forms the base of these dishes, features the required electrical and optical properties and serves as ground electrode. In contrast to gold, ITO is suitable for fluorescence microscopy, allows live-cell imaging, and can be combined with various functionalization options to support cell growth if needed (Luo et al., 2008; Shah et al., 2009). The ability to carry out live-cell imaging prior to cell lysis, not only allows studying

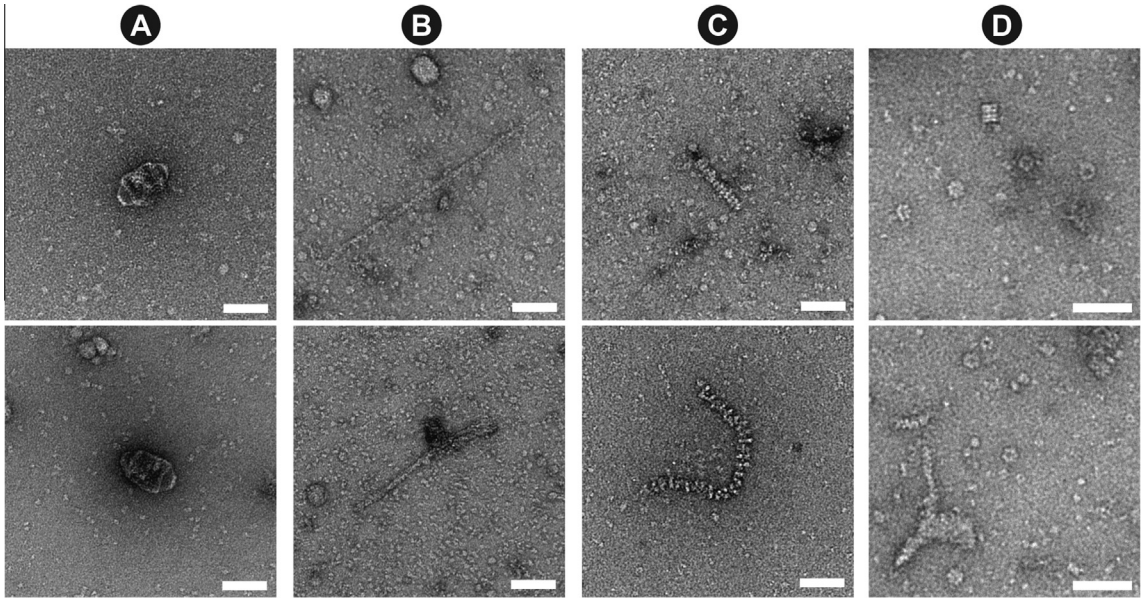

Fig.4. Examples of distinctive structures observed in negatively stained cell lysates of individual cells. Negative stain: 2% UA. Scale bars 50 nm. (A) Structures that resemble vault organelles, which are large ribonucleoprotein particles found predominantly in the eukaryotic cytoplasm (Kedersha et al., 1990). (B) Helical structures that have the shape and dimensions of actin filaments (Aebi et al., 1986). (C) Examples of other less abundant structures observed in the lysate of individual cells. These resemble (top) the CplXAP complex (Ortega et al., 2004) and (bottom) nucleoprotein filaments (Sehorn et al., 2004). (D) More detailed view of the frequently observed ring-like structures shown in F. These have variable dimensions and resemble top views of Hsp60 (De Carlo et al., 2008) and the 20s proteasome (Cascio et al., 2002); the rectangular structure in the top image resembles a side view of one of the latter complexes.

biological processes, but also enables lysis to be initiated at a defined time-point by means of an optical feedback; for example, a target cell in a specific state can be identified and selected by fluorescence signals of genetically labeled proteins.

Microfluidic chips with fixed electrodes often suffer from bubble formation due to electrolysis. In the flexible-electrode setup described here, sample aspiration and downstream processing were not affected by electrolysis, and there were no signs of bubbles inside the capillary. Furthermore, microfluidic chips with embedded electrodes depend on cells being in suspension and are not well suited to study adherent eukaryotic cells, which must be detached before lysis.

Biological processes involving proteins elapse within time frames of milliseconds to days (Souchelnytskyi, 2005). This makes the total lysis time an important parameter for cellular dynamics studies. As the method presented here combines fast electrical lysis ($\leqslant$1 ms) with rapid sample loading ($\leqslant$400 ms), the described technique offers a temporal resolution that is suitable to study dynamic processes in protein networks of single cells.

The complete detachment and disruption of the cells, observed after sample aspiration (Fig. 2B and C and Supp. Fig. 2B–F), was most likely due to the additional shear forces occurring during the aspiration process. The combination of electrical pulses and mechanical forces, allows applying relatively mild conditions for electrical lysis (low pulse amplitudes and short pulses) in comparison to those reported previously (Han et al., 2003; Nashimoto et al., 2007).

The preservation of the native protein structure and supramolecular assemblies is crucial for the subsequent visual analysis in EM. FEA predicts elevated temperatures on time scales $\leqslant$1 ms (Fig. 3B and supp. Fig. 4) and indicates that thermal protein denaturation is unlikely to occur. All our experimental data corroborate these findings: Quantitative assays using HRP did not show a significant degradation of enzyme activity at the conditions used to lyse individual cells (Fig. 3C). Furthermore, experiments with synthetic actin filaments only showed structural effects at voltages exceeding the ones used for lysis (Supp. Fig. 6).

Negative-stain TEM revealed a variety of cellular components, such as membrane patches, filaments and other particles (Figs. 2 and 4), and indicates the structural preservation of the observed cellular components. No signs of protein aggregation were observed (compare to supp. Fig. 6 D). Due to the unique and distinct shape of several particles, assumptions about their identity can be made directly from the raw images, e.g., for the vault organelles (Kedersha et al., 1990). Future template matching algorithms must include scoring algorithms for quantitative analysis (Beck et al., 2009, 2011; Best et al., 2007) or complementary, labeling procedures (Giss et al., manuscript in preparation) can be employed. Although the aspects of protein structure and protein complex preservation have to be further consolidated and the recovery of sample constituents has to be improved in the future, the TEM images clearly demonstrate the potential of this method to prepare the lysate of a single cell for a visual analysis in negative-stain TEM. Furthermore, single cell lysis of adherent eukaryotic cells is also of great interest for other analysis methods, such as mass spectrometry (Aebersold and Mann, 2003) or reverse-phase protein arrays (RPPA) (Dernick et al., 2011). The application of our lysis method for the detection of actin by RPPA is shown in Supplementary Fig. 7.

The "lyse and spread" approach for visual analysis of eukaryotic cells presented here is envisaged to complement classical methods, such as cryo-ET or mass spectroscopy. In comparison to cryo-ET of whole vitrified cells or cellular sections, the here presented approach does not provide information about the 3D arrangement of the proteome. In addition, the excellent preservation capabilities of vitrification have to be replaced by mild and physiological conditions during sample preparation and eventually supported by crosslinking procedures. On the other hand, the "lyse and spread" method, focusing particularly on the cytosolic fraction, has several advantages: (i) Adherent eukaryotic cells can be studied; (ii) the proteins can be prepared by negative staining to obtain a higher SNR; and (iii) the physical segmentation renders the cell components directly accessible for separation and labeling experiments (Giss et al., in preparation). In contrast to mass spectroscopy, mass

determination by STEM is less accurate and the visual analysis by TEM is less high-throughput amenable. However, the single molecule detection limit of the EM allows low-abundance proteins and protein complexes to be studied. Moreover, EM provides additional structural information and facilitates the study of large protein assemblies.

The presented single cell lysis method is only a first step toward the global approach described above as "lyse and spread visual proteomics". Currently, a limiting step is the low transfer efficiency of the cell lysate onto the EM grid, involving several blotting and washing steps. Therefore, the combination with methods exhibiting higher transfer efficiency will be beneficial in order to obtain a more complete access to the proteome. For example, the use of a microfluidic sample-conditioning device, combined with lossless micropatterning of the sample onto an EM grid, could be a suitable solution as shown by Kemmerling et al. (2012).

5. Conclusion and outlook

The system presented here allows single-cell lysis to be performed in less than a millisecond and to aspirate the cellular components into a microcapillary within a few hundred milliseconds for further preparation and subsequent analysis. The combination of this setup with an optical system facilitates live imaging and the evaluation of lysis and sample loading. The system is compatible with standard adherent-cell culturing methods and tools, and can potentially also be applied to biological tissues. Moreover, the system can be easily adapted to different sample carriers, which facilitates the use with additional or alternative analysis techniques such as reverse-phase protein arrays (Supp. Fig. 7).

In combination with a lossless sample deposition onto the EM grids and optional procedures for crosslinking, protein separation and labeling this method for single cell lysis offers the potential for targeted and quantitative visual proteomics studies on eukaryotic single cells.

Acknowledgments

We thank Andreas Engel for his inspiring ideas and support, the workshop of the Biozentrum of the University Basel for their aid and Shirley Müller for carefully reading the manuscript and expert discussions. The project was financially supported by the SNF (NSX1003, granted to T.B.), SystemsX.ch (CINA, granted to H.S., co-PI is A.H.) and the NCCR Nanoscience.

Appendix A. Supplementary data

Supplementary data associated with this article can be found, in the online version, at http://dx.doi.org/10.1016/j.jsb.2013.06.012.

References

Aebersold, R., Mann, M., 2003. Mass spectrometry-based proteomics. Nature 422, 198–207.
Aebi, U., Millonig, R., Salvo, H., Engel, A., 1986. The three dimensional structure of the actin filament revisited. Ann. NY Acad. Sci. 483, 100–119.
Amantonico, A., Oh, J.Y., Sobek, J., Heinemann, M., Zenobi, R., 2008. Mass spectrometric method for analyzing metabolites in yeast with single cell sensitivity. Angew. Chem. Int. Ed. Engl. 120, 5462–5465.
Bantscheff, M., Schirle, M., Sweetman, G., Rick, J., Kuster, B., 2007. Quantitative mass spectrometry in proteomics: a critical review. Anal. Bioanal. Chem. 389, 1017–1031.
Beck, M., Malmström, J.A., Lange, V., Schmidt, A., Deutsch, E.W., et al., 2009. Visual proteomics of the human pathogen *Leptospira interrogans*. Nat. Methods 6, 817–823.
Beck, M., Topf, M., Frazier, Z., Tjong, H., Xu, M., et al., 2011. Exploring the spatial and temporal organization of a cell's proteome. J. Struct. Biol. 173, 483–496.
Best, C., Nickell, S., Baumeister, W., 2007. Localization of protein complexes by pattern recognition. Methods Cell Biol. 79, 615–638.
Brown, R.B., Audet, J., 2008. Current techniques for single-cell lysis. J. R. Soc. Interface 5, S131–S138.
Cascio, P., Call, M., Petre, B.M., Walz, T., Goldberg, A.L., 2002. Properties of the hybrid form of the 26S proteasome containing both 19S and PA28 complexes. EMBO J. 21, 2636–2645.
Chattopadhyay, K., Mazumdar, S., 2000. Structural and conformational stability of horseradish peroxidase: effect of temperature and pH. Biochemistry 39, 263–270.
De Carlo, S., Boisset, N., Hoenger, A., 2008. High-resolution single-particle 3D analysis on GroEL prepared by cryo-negative staining. Micron 39, 934–943.
Dernick, G., Obermüller, S., Mangold, C., Magg, C., Matile, H., et al., 2011. Multidimensional profiling of plasma lipoproteins by size exclusion chromatography followed by reverse-phase protein arrays. J. Lipid Res. 52, 2323–2331.
Diebolder, C.A., Koster, A.J., Koning, R.I., 2012. Pushing the resolution limits in cryo electron tomography of biological structures. J. Microsc. 248, 1–5.
Eldar, A., Elowitz, M.B., 2010. Functional roles for noise in genetic circuits. Nature 467, 167–173.
Engel, A., 2009. Scanning transmission electron microscopy: biological applications. In: Hawkes, P. (Ed.), Advances in Imaging and Electron Physics. Academic Press, Burlington, pp. 357–386.
Engel, A., 2010. Assessing biological samples with scanning probes. In: Gräslund, A., Rigler, R., Widengren, J. (Eds.), Single Molecule Spectroscopy in Chemistry, Physics and Biology. Springer, Berlin Heidelberg, pp. 417–431.
Fiehn, O., 2001. Combining genomics, metabolome analysis, and biochemical modelling to understand metabolic networks. Comp. Funct. Genomics 2, 155–168.
Flatz, L., Roychoudhuri, R., Honda, M., Filali-Mouhim, A., Goulet, J.-P., et al., 2011. Single-cell gene-expression profiling reveals qualitatively distinct CD8 T cells elicited by different gene-based vaccines. Proc. Nat. Acad. Sci. 108, 5724–5729.
Fox, M., Esveld, D., Valero, A., Luttge, R., Mastwijk, H., et al., 2006. Electroporation of cells in microfluidic devices: a review. Anal. Bioanal. Chem. 385, 474–485.
Han, F., Wang, Y., Sims, C.E., Bachman, M., Chang, R., et al., 2003. Fast electrical lysis of cells for capillary electrophoresis. Anal. Chem. 75, 3688–3696.
Henderson, G.P., Gan, L., Jensen, G.J., 2007. 3-D ultrastructure of *O. tauri*: electron cryotomography of an entire eukaryotic cell. PLoS ONE 2, e749.
Kalisky, T., Blainey, P., Quake, S.R., 2011. Genomic analysis at the single-cell level. Annu. Rev. Genet. 45, 431–445.
Kedersha, N.L., Miquel, M.C., Bittner, D., Rome, L.H., 1990. Vaults. II. Ribonucleoprotein structures are highly conserved among higher and lower eukaryotes. J. Cell Biol. 110, 895–901.
Kemmerling, S., Ziegler, J., Schweighauser, G., Arnold, S.A., Giss, D., et al., 2012. Connecting μ-fluidics to electron microscopy. J. Struct. Biol. 177, 128–134.
Luo, W., Westcott, N.P., Pulsipher, A., Yousaf, M.N., 2008. Renewable and optically transparent electroactive indium tin oxide surfaces for chemoselective ligand immobilization and biospecific cell adhesion. Langmuir 24, 13096–13101.
Mader, A., Elad, N., Medalia, O., 2010. Cryoelectron tomography of eukaryotic cells. Methods Enzymol. 483, 245–265.
Medalia, O., Weber, I., Frangakis, A.S., Nicastro, D., Gerisch, G., et al., 2002. Macromolecular architecture in eukaryotic cells visualized by cryoelectron tomography. Science 298, 1209–1213.
Movahed, S., Li, D., 2011. Microfluidics cell electroporation. Microfluid. Nanofluid. 10, 703–734.
Nashimoto, Y., Takahashi, Y., Yamakawa, T., Torisawa, Y., Yasukawa, T., et al., 2007. Measurement of gene expression from single adherent cells and spheroids collected using fast electrical lysis. Anal. Chem. 79, 6823–6830.
Nickell, S., Kofler, C., Leis, A.P., Baumeister, W., 2006. A visual approach to proteomics. Nat. Rev. Mol. Cell Biol. 7, 225–230.
Ortega, J., Lee, H.S., Maurizi, M.R., Steven, A.C., 2004. ClpA and ClpX ATPases bind simultaneously to opposite ends of ClpP peptidase to form active hybrid complexes. J. Struct. Biol. 146, 217–226.
Picotti, P., Bodenmiller, B., Mueller, L.N., Domon, B., Aebersold, R., 2009. Full dynamic range proteome analysis of *S. cerevisiae* by targeted proteomics. Cell 138, 795–806.
Raj, A., van Oudenaarden, A., 2008. Nature, nurture, or chance: stochastic gene expression and its consequences. Cell 135, 216–226.
Sehorn, M.G., Sigurdsson, S., Bussen, W., Unger, V.M., Sung, P., 2004. Human meiotic recombinase Dmc1 promotes ATP-dependent homologous DNA strand exchange. Nature 429, 433–437.
Shah, S.S., Howland, M.C., Chen, L.-J., Silangcruz, J., Verkhoturov, S.V., et al., 2009. Micropatterning of proteins and mammalian cells on indium tin oxide. ACS Appl. Mater. Interfaces 1, 2592–2601.
Souchelnytskyi, S., 2005. Bridging proteomics and systems biology: what are the roads to be traveled? Proteomics 5, 4123–4137.
Wang, D., Bodovitz, S., 2010. Single cell analysis: the new frontier in 'omics'. Trends Biotechnol. 28, 281–290.
Westerhoff, H.V., 2011. Systems biology left and right. Methods Enzymol. 500, 3–11.
Zong, C., Lu, S., Chapman, A.R., Xie, X.S., 2012. Genome-wide detection of single-nucleotide and copy-number variations of a single human cell. Science 338, 1622–1626.